

Optical Fiber Refractive Index Profile Synthesis from Near Field

A. C. Boucouvalas and X. Qian

Multimedia Communications Research Group, School of Design, Engineering and Computing,
Bournemouth University, Fern Barrow, Poole, BH12 5BB, UK,
{ tboucouv, qxian }@bournemouth.ac.uk

Abstract – A new and accurate refractive index profile synthesis method for optical waveguides is demonstrated using the transmitted near electric field data. This method is based on an inverse transmission line technique. From Maxwell's equations, we derive a transmission line equivalent circuit for the refractive index profile of a cylindrical dielectric waveguide. We demonstrate how to use this model and carry out the inverse problem and synthesize the exact refractive index profile numerically from near field data. Based on knowledge of the electric field, we demonstrate results of numerical reconstruction of step index, parabolic, and segmented optical fibre refractive index profiles. The accuracy of the reconstructed waveguides is examined numerically.

I. INTRODUCTION

It is of fundamental importance to be able to determine the refractive index profile of optical waveguides, as their main characteristics, bandwidth, spot size, single-mode propagation conditions, and interwaveguide coupling coefficients can all be related to their refractive index profiles. Profile measurement, however, is generally very difficult due to small dimensions and low refractive index differences. A number of techniques, [1], have been proposed for determining the refractive index distribution of optical fibres from the propagation mode near field, and the most well known rely on the seminal theoretical work by Morishita, [2]. Reference [2] relies on an inverse solution of the scalar wave equation for the refractive index profile. In [1], the measurement of the near field intensity is improved using a scanning optical microscopy technique rather than conventional optics. Improvements from [2], have been recently reported in [3], which is a robust method to noise and errors, and non-iterative, but reported for planar waveguides.

We have shown that transmission line techniques can be applied in optical fibres and can determine exactly the mode propagation constants [4], and cutoff wavelengths of waveguide modes [5]. In general from knowledge of the refractive index, complete waveguide characterisation can be achieved, including mode field plots using this powerful technique, [6].

In this paper we are dealing with the inverse problem. The problem we address can be stated as follows: Given that the guided mode near field is known, can we use the transmission line principles in order to determine the refractive index profile? It is well known that inverse problems are much more difficult to solve, they often are non-linear, and suffer from stability problems. We offer a new simple technique which does not require direct inversion of the scalar wave equation, but uses a recursive algorithm which reconstructs the refractive

index directly with radius. The following section describes the basic theory our technique is based upon.

II. FORWARD SOLUTION

We divide an optical waveguide into a large number of homogeneous cylindrical layers of thickness δr , permittivity ϵ , permeability μ and conductivity σ in Fig.1.

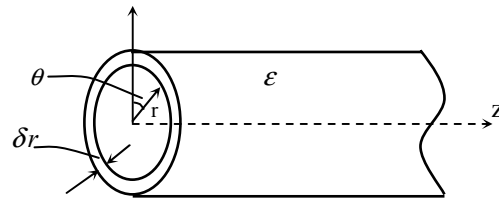


Figure.1. Homogeneous cylindrical layer

The E and H components of Maxwell's equations for any such layer can be written as:

$$\left. \begin{aligned} \beta r E_{\theta} - l E_z &= \omega \mu r H_r \\ l H_z - \beta r H_{\theta} &= (\omega \epsilon - j \sigma) r E_r \\ \frac{\partial(\omega \mu r H_r)}{\partial r} &= -j \omega \mu (l H_{\theta} + \beta r H_z) \end{aligned} \right\} \quad (1)$$

$$\left. \begin{aligned} \frac{\partial[(\omega \epsilon - j \sigma) r E_r]}{\partial r} &= -(\sigma + j \omega \epsilon)(l E_{\theta} + \beta r E_z) \\ \frac{\partial(l H_{\theta} + \beta r H_z)}{\partial r} &= -\frac{\gamma^2}{j \omega \mu} \omega \mu r H_r + \beta H_z - \frac{l}{r} H_{\theta} \\ \frac{\partial(l E_{\theta} + \beta r E_z)}{\partial r} &= -\frac{\gamma^2}{\sigma + j \omega \epsilon} (\omega \epsilon - j \sigma) r E_r + \beta E_z - \frac{l}{r} E_{\theta} \end{aligned} \right\} \quad (2)$$

$$\text{where } \gamma^2 = \beta^2 + \left(\frac{l}{r}\right)^2 - \omega^2 \mu \omega + j \omega \mu \sigma$$

We restrict our analysis to the case $\sigma = 0, \mu = \mu_0, \epsilon = n^2 \epsilon_0$, where n is the refractive index of the layer at distance r from the axis.

We define the following variable voltages and currents:

$$\left. \begin{aligned}
 V_s &= \frac{V_M}{\sqrt{n}} + V_E \sqrt{n} && \text{(sum)} \\
 V_d &= \frac{V_M}{\sqrt{n}} - V_E \sqrt{n} && \text{(difference)} \\
 I_s &= I_M \sqrt{n} + \frac{I_E}{\sqrt{n}} && \text{(sum)} \\
 I_d &= I_M \sqrt{n} - \frac{I_E}{\sqrt{n}} && \text{(difference)}
 \end{aligned} \right\} \quad (3)$$

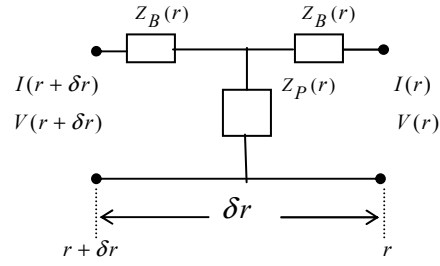


Figure.2. Equivalent circuit of a dielectric waveguide

where

$$V_M = \frac{lH_\theta + \beta r H_z}{jF} Z_0 \quad \text{(magnetic voltage)}$$

$$V_E = \frac{lE_\theta + \beta r E_z}{F} Z_0 \quad \text{(electric voltage)}$$

$$I_E = \omega \epsilon_0 n^2 r E_r \quad \text{(electric current)}$$

$$Z_0 = 120\pi \text{ the free space impedance, } F = \frac{(\beta r)^2 + l^2}{r}$$

After some algebra, (1) and (2) can be transformed into:

$$\left. \begin{aligned}
 \frac{\partial V_s}{\partial r} &= \frac{-\gamma_s^2}{j\omega \epsilon_0 n F} I_s \\
 \frac{\partial I_s}{\partial r} &= -j\omega \epsilon_0 n F V_s
 \end{aligned} \right\} \quad (4)$$

$$\left. \begin{aligned}
 \frac{\partial V_d}{\partial r} &= \frac{-\gamma_d^2}{j\omega \epsilon_0 n F} I_d \\
 \frac{\partial I_d}{\partial r} &= -j\omega \epsilon_0 n F V_d
 \end{aligned} \right\} \quad (5)$$

where $\gamma_s^2 = \beta^2 + (\frac{l}{r})^2 - n^2 k_0^2 \mp \frac{2nk_0\beta l}{(\beta r)^2 + l^2}$ (- for HE, + for EH modes).

Equations (4) and (5) represent two independent transmission lines with voltages V_s, V_d and currents I_s, I_d . The corresponding characteristic impedances are:

$$\left. \begin{aligned}
 Z_s &= \frac{\gamma_s}{j\omega \epsilon_0 n F} \\
 Z_d &= \frac{\gamma_d}{j\omega \epsilon_0 n F}
 \end{aligned} \right\} \quad (6)$$

The above equations are recognized as the well known transmission line equations with the solution represented by the following electric circuit Fig. 2.

$$\left. \begin{aligned}
 Z_B &= Z_d \tanh(\gamma_d \frac{\delta r}{2}) \\
 Z_P &= \frac{Z_d}{\sinh(\gamma_d \delta r)}
 \end{aligned} \right\} \quad (7)$$

where δr is the length of the transmission line.

Since δr is infinitesimal, ($\frac{\delta r}{r} \ll 1$), we finally have

$$\left. \begin{aligned}
 Z_B &= \frac{1}{2} (\delta r)^2 \gamma_d^2 Z_P \\
 Z_P &= \frac{Z_0}{jn r \delta r k_0 (\beta^2 + (\frac{l}{r})^2)}
 \end{aligned} \right\} \quad (8)$$

$$\text{with } \gamma_{sd}^2 = \beta^2 + (\frac{l}{r})^2 - n^2 k_0^2 \mp \frac{2nk_0\beta l}{(\beta r)^2 + l^2}$$

Normalizing (8) with respect to K_0 gives:

$$\left. \begin{aligned}
 \bar{Z}_B &= \frac{1}{2} (\delta \bar{r})^2 \bar{\gamma}_d^2 \bar{Z}_P \\
 \bar{Z}_P &= \frac{Z_0}{jn \bar{r} \delta \bar{r} (\bar{\beta}^2 + (\frac{l}{\bar{r}})^2)}
 \end{aligned} \right\} \quad (9)$$

where $\bar{r} = r k_0, \delta \bar{r} = \delta r k_0, \bar{\beta} = \frac{\beta}{k_0}$

$$\bar{\gamma}_d^2 = \gamma_d^2 / k_0^2 = \bar{\beta}^2 + (\frac{l}{\bar{r}})^2 - n^2 \mp \frac{2n\bar{\beta}l}{(\bar{\beta}\bar{r})^2 + l^2}$$

$$\bar{Z}_P = Z_P \times K_0, \bar{Z}_B = Z_B \times K_0$$

From the above equations, we can derive the Electric current I and Electric field E_r . We know that:

$$\left. \begin{aligned}
 V_{HE} &= \frac{V_M}{\sqrt{n(r)}} + V_E \sqrt{n(r)} \\
 V_{EH} &= \frac{V_M}{\sqrt{n(r)}} - V_E \sqrt{n(r)}
 \end{aligned} \right\} \quad (10)$$

$$\left. \begin{aligned} I_{HE} &= I_M \sqrt{n(r)} + \frac{I_E}{\sqrt{n(r)}} \\ I_{EH} &= I_M \sqrt{n(r)} - \frac{I_E}{\sqrt{n(r)}} \end{aligned} \right\} \quad (11)$$

We wish to determine the E/M field of the HE mode in terms of I_{HE} and V_{HE} variables, we can set $I_{HE} = V_{HE} = 0$ when the HE modes are of interest. This implies that

$$\left. \begin{aligned} I_M \sqrt{n(r)} &= \frac{I_E}{n(r)} \\ \frac{V_M}{\sqrt{n(r)}} &= V_E \sqrt{n(r)} \end{aligned} \right\} \quad (12)$$

Substituting into (10) and (11), we have:

$$\left. \begin{aligned} V_{HE} &= 2V_E \sqrt{n(r)}, \quad I_{HE} = 2I_M \sqrt{n(r)} \\ V_{HE} &= 2 \frac{V_M}{\sqrt{n(r)}}, \quad I_{HE} = 2 \frac{I_E}{\sqrt{n(r)}} \end{aligned} \right\} \quad (13)$$

Note that I_{HE} , V_{HE} are also referred to as I_s , V_s respectively.

Hence:

$$\left. \begin{aligned} V_E &= \frac{V_s}{2\sqrt{n(r)}}, \quad I_M = \frac{I_s}{2\sqrt{n(r)}} \\ V_M &= \frac{V_s \sqrt{n(r)}}{2}, \quad I_E = \frac{I_s \sqrt{n(r)}}{2} \\ I_E &= \omega \epsilon_0 n^2(r) r E_r \end{aligned} \right\} \quad (14)$$

Hence:

$$E_r = \frac{I_E}{\omega \epsilon_0 n^2 r} = \frac{Z_0 I_E}{k_0 n^2(r) r} = \frac{Z_0 I_E}{n^2(r) \bar{r}} \quad (15)$$

Therefore if we already know the refractive index as a function of radius, we can use the (15) to plot the Electric field, E_r , precisely.

III. INVERSE PROBLEM

For determining the refractive index profile from knowledge of E_r , we assume the following boundary condition: At $r = \infty$, we assume $n = n_2$ (silica refractive index).

The equivalent circuit for a cylindrical thin layer, Fig.1, of constant refractive index n and thickness $\delta_{\bar{r}}$ at distance \bar{r} from the core is represented as an electric circuit in Fig. 3:

At $r = \infty$, we know $Z_{prev} = 0$ and $n(\infty) = n_2$, From circuit theory, we may use the following recursive relation to determine the values of $Z_{P,n}$, $Z_{B,n}$ and $Z_{prev} = Z_n$.

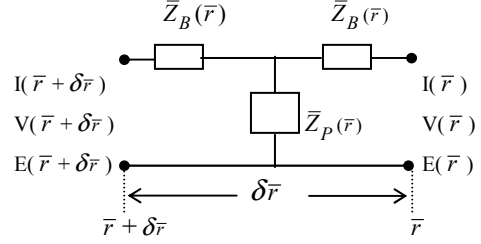


Figure.3. Equivalent circuit for a cylindrical thin layer at constant refractive index n and thickness $\delta_{\bar{r}}$ at distance \bar{r} from the core

$$\left. \begin{aligned} \bar{Z}_n &= \frac{(\bar{Z}_{n-1} + \bar{Z}_{B,n}) \bar{Z}_{P,n}}{\bar{Z}_{n-1} + \bar{Z}_{B,n} + \bar{Z}_{P,n}} + \bar{Z}_{B,n} \\ \bar{Z}_{B,n} &= \frac{1}{2} \bar{\gamma}^2 \delta_{\bar{r}}^2 \bar{Z}_P \\ \bar{Z}_{P,n} &= \frac{Z_0}{n(r) \bar{r} \delta_{\bar{r}} (\bar{\beta}^2 + \frac{l^2}{\bar{r}^2})} \end{aligned} \right\} \quad (16)$$

$$\text{where } \bar{\gamma}^2 = \bar{\beta}^2 + \frac{l^2}{\bar{r}^2} - n^2(r) - \frac{2\bar{\beta} \ln(r)}{(\bar{\beta}^2 \bar{r}^2 + l^2)}.$$

We know that $\bar{\beta}$ is the effective refractive index and for typical waveguides lies between n_1 and n_2 . For the time being, we also assume we have full knowledge of $\bar{\beta}$.

We also know λ_0 , \bar{r} , $\delta_{\bar{r}}$, $n(\infty) = n_2$.

Hence $I(\bar{r} + \delta_{\bar{r}})$, $V(\bar{r} + \delta_{\bar{r}})$ can be calculated for any radius. Hence we can work out $n(\bar{r})$ as follows:

$$\left. \begin{aligned} I_s &= \frac{2I_E}{\sqrt{n}} \\ E_{\bar{r}}(\bar{r}) &= \frac{I_E(\bar{r}) Z_0}{n^2 \bar{r}} \end{aligned} \right\} \quad (17)$$

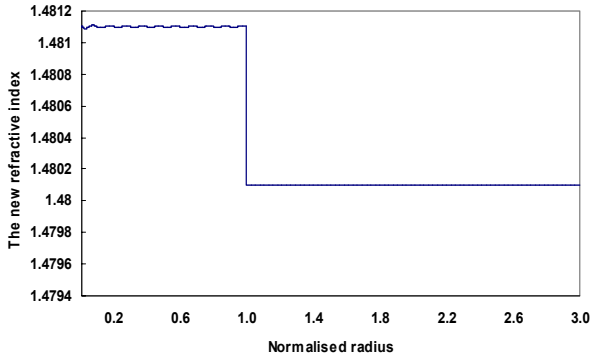
and finally $E(\bar{r}) = \frac{I_s(\bar{r}) Z_0}{2n^{3/2} \bar{r}}$ and hence

$$n(\bar{r}) = \left(\frac{I_s(\bar{r}) Z_0}{2E(\bar{r}) \bar{r}} \right)^{2/3} \quad (18)$$

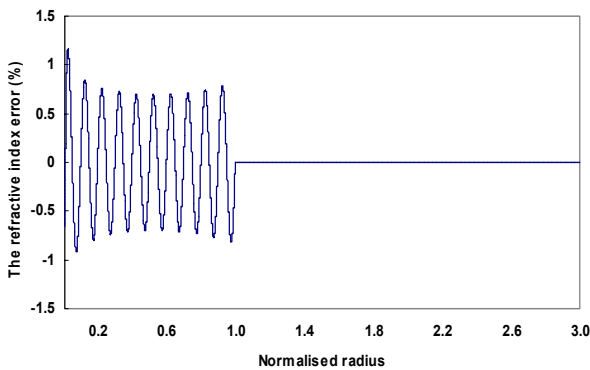
Since we know $E(\bar{r})$ and $I_s(\bar{r})$, hence we can calculate $n(\bar{r})$.

IV. NUMERICAL RESULTS

Fig. 4(a) shows the reconstructed refractive index profile of a step index optical fibre of refractive index $n_1=1.4811$ and $n_2=1.4801$. In order to compare its accuracy with the original refractive index Fig. 4 (b) shows the % error versus the normalised radius.



(a)



(b)

Figure.4. (a) The reconstructed refractive index using (18).
(b) The % max. error in refractive index difference due to ripple.

$$(\max(n_{exact} - n_{reconstructed}) / n \%)$$

The error in refractive index oscillates about the exact value in the core. The error in the cladding is zero. The oscillations in the core depend on the number of layers we use for the reconstruction of the index as shown in Fig.5.

We can see in Fig. 5 that less than 1% error due to the ripple in Δn can be achieved with up to 30,000 layers. This could be due to the use of the approximations (8) instead of the exact (6), as well as the fact that the layer must be very thin in order to apply this theory accurately.

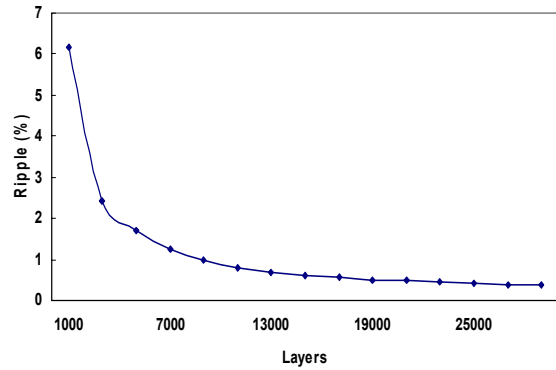


Figure.5. The refractive index difference, maximum % ripple (error) of the synthesized refractive index versus number of layers.

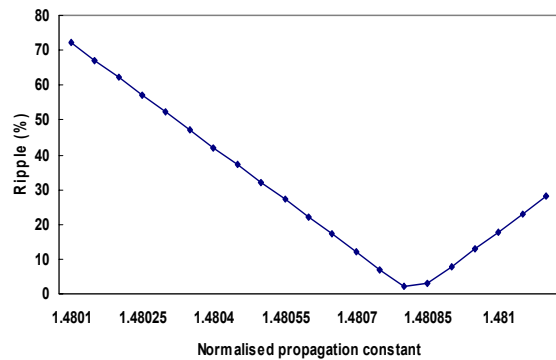


Figure.6. The refractive index difference, maximum % ripple (error) of the synthesized refractive index versus values for $\bar{\beta}$ offset from exact.

Fig.6 shows the effect of inaccuracies in $\bar{\beta}$ on the ripple in the reconstructed Δn . We observe that the ripple increases with use the incorrect $\bar{\beta}$. The min. error occurs at the exact $\bar{\beta}$. However, this is not a problem if we do not know it, since we can simply start the reconstruction with $\bar{\beta} = n_2$ and repeat the process with a $\bar{\beta}$ change within $n_2 \leq \bar{\beta} \leq n_1$ until the ripple is minimum, Fig.6. At this minimum ripple point we have the exact $\bar{\beta}$, and the reconstructed refracted index is also exact.

Fig. 7, shows an example refractive index reconstruction for a segmented core fibre. The remarkable accuracy of the reconstruction is demonstrated in Fig. 8, where the ripple % error in Δn is shown. The % error is less than 1.6%.

Fig. 9 is another example reconstruction of a parabolic refractive index profile and Fig.10 shows the % error in Δn which is less than 0.06%. Clearly the parabolic is less demanding in reconstruction than a step index profile.

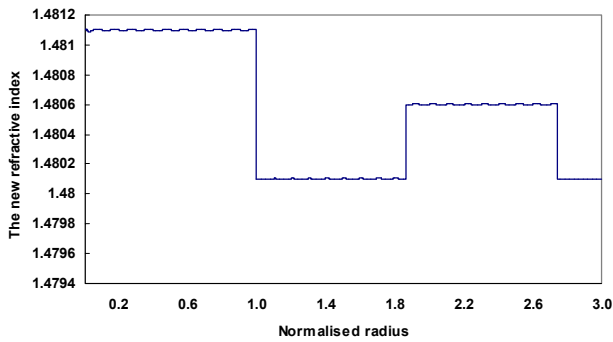


Figure.7. Example of a reconstructed segmented core refractive index profile from the electric field

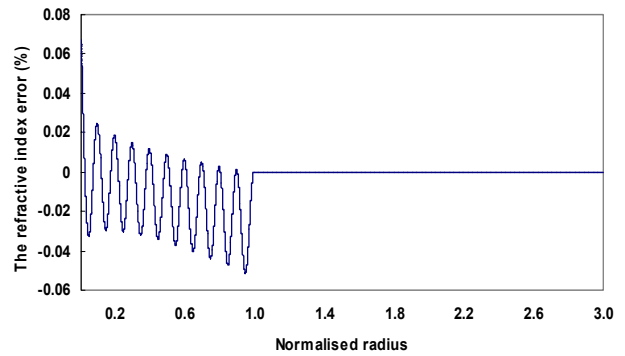


Figure.10. The refractive index difference, maximum % ripple (error) of the synthesized parabolic refractive index of Fig. 9.

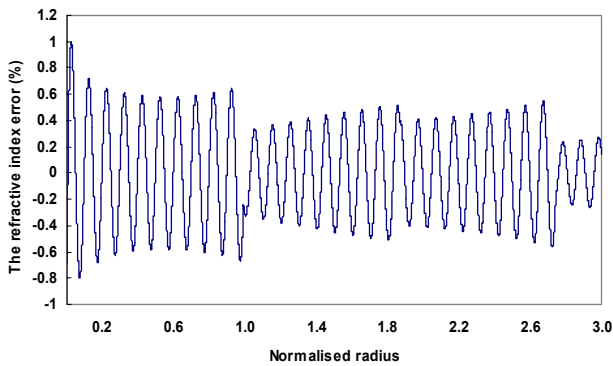


Figure.8. The refractive index difference, maximum % ripple (error) of the synthesized segmented core refractive index of Fig. 7.

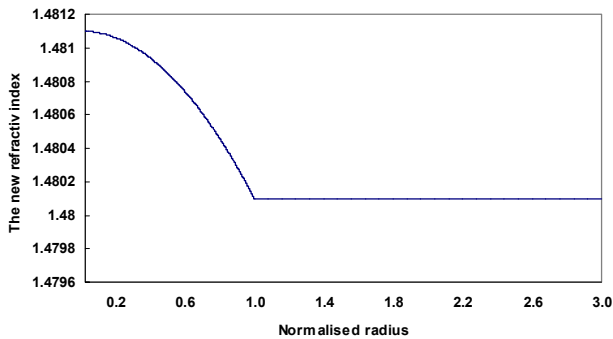


Figure.9. A parabolic refractive index reconstruction from the near field.

V. CONCLUSIONS

In this paper, a new and accurate refractive index profile synthesis technique has been developed. The method uses inverse transmission line principles and relies on the modelling of a thin uniform cylindrical layer of an optical fibre to a transmission line circuit. The method requires knowledge of the near field of the optical fibre and the reconstruction is theoretically exact. Simulation results demonstrate the potential of this new method for reconstructing arbitrary refractive index profiles.

REFERENCES

- [1] L. Dhar, H. J. Lee, E. J. Laskowski, S. K. Buratto, H. M. Presby, C. Narayanan, C.C. Bahr, P.J. Anthony, M. J. Cardillo: "Refractive index profiling of optical waveguides using near-field scanning optical microscopy", OFC 1996, paper FB-5, pp.303-304.
- [2] K. Morishita: "Refractive-Index-Profile Determination of Single Mode Optical Fibres by a Propagation-Mode Near Field Scanning Technique" IEEE J. Lightwave technology Vol LT-1, No 3, Sept. 1983, pp.445-449.
- [3] Jin-Hong Lin and Cha'o-Kuang Chen "An inverse Algorithm to Calculate the refractive Index Profiles of Periodically Segmented Waveguides from the Measured Near-Field Intensities" IEEE J. Lightwave Technology, Vol.20, No 1, Jan 2002, pp.58-64.
- [4] C D Papageorgiou and AC Boucouvalas: "Propagation constants of cylindrical dielectric waveguides with arbitrary refractive index profile, using the 'Resonance' technique". Electronics Letters, Vol 18, No 18, 2 September 1982, pp.768-788
- [5] A C Boucouvalas and C D Papageorgiou: Cutoff frequencies in optical fibres of arbitrary refractive index profile using the 'resonance' technique. IEEE Journal of Quantum Electronics, Vol QE-18, No 12, Dec. 1982, pp. 2027-2031
- [6] A C Boucouvalas and S C Robertson: "Optical waveguide transverse transmission line equations and their use in determining mode properties". JOERS Advanced Fibre Measurement Symposium, National Physical Laboratories, London, 10 September 1985.